Original Manuscript

AAHS AMERICAN ASSOCIATION FOR HAND SURGERY

HAND
1–7


Article reuse guidelines:
sagepub.com/journals-permissions
DOI: 10.1177/15589447221122825
journals.sagepub.com/home/HAN

A Volar Locking Plate With Fossa Specific Fixation Provides Comparable Stability Between Articular and Nonarticular Cadaveric Models of Distal Radius Fracture

John J. Heifner[1], Natalia D. McIver[2], Christina Salas[2], and Deana M. Mercer[3]

Abstract

Background: Distal radius fractures often present with a 3-part articular fragmentation pattern, with separation of the dorsal and volar lunate fossa. The column concept of distal radius fixation addresses the importance of stabilizing both the scaphoid fossa lateral column and the lunate fossa intermediate column. Recent evidence strengthens the value of immediate postoperative mobilization. Satisfactory outcomes following these protocols are predicated on volar locking plates (VLPs) providing adequate stability to the fracture repair. We hypothesize that a VLP which individually supports both lateral and intermediate distal radius columns may provide comparable stability between articular and non-articular cadaveric fracture models under parameters meant to simulate postoperative loading. **Methods:** Eleven cadaveric matched pair specimens were randomized to receive a simulated AO Type A2 non-articular distal radius fracture on one side with an AO Type C3 articular fracture on the contralateral side. Stiffness during cyclic loading was compared between fracture groups. A matched-paired Student t-test was used to determine statistical significance ($P = .05$). **Results:** There were no significant differences ($P = .35$) in stiffness between the articular models (mean 370.0 N/mm, +/-93.5) and the non-articular models (360.4 N/mm, +/-60.0) of distal radius fracture. **Conclusion:** A VLP that individually supports the scaphoid and lunate fossa with fixed angle subchondral support may provide comparable fixation strength with resistance to displacement between articular and non-articular fracture patterns. The current results suggest that fossa-specific VLP fixation in articular fractures can maintain construct stability during postoperative loading.

Keywords: articular distal radius fracture, distal radius columns, distal radius fracture, lunate fossa, volar locking plate

Introduction

The incidence of distal radius fractures (DRFs) is expected to rise as the population of older adults increases.[1,2] The current guidelines from the American Academy of Orthopaedic Surgeons (AAOS) recommend conservative treatment for displaced DRF in adults over 65 years of age.[3] Recent reports describe an increasing rate of surgical treatment in DRF.[4,5] In part, this may be due to improved clinical outcomes in DRF after the introduction of the volar locking plate (VLP), which is currently the most common form of surgical treatment.[6-8] Volar locking plates have shown efficacy in addressing a variety of common articular fracture patterns.[9-11]

Distal radius fractures present with articular surface involvement in approximately 50% of cases, commonly with a 3-fragment pattern involving the scaphoid and lunate fossa as described by Melone.[5,12,13] There is recent evidence that within AO type C articular fracture patterns, the C3 subset which has more than 2 articular fragments, is most common.[14] Fragmentation of the articular surface may reduce the stability that is provided by a VLP, as the number of fixation points per individual fragment is reduced. Volar locking plate produce stability by creating a scaffold underneath the subchondral bone to support the articular surface of the distal fragment(s)—this is referred to as a raft construct.

[1]St. George's University School of Medicine, Great River, NY, USA
[2]University of New Mexico School of Engineering, Albuquerque, NM, USA
[3]University of New Mexico Health Sciences Center, Albuquerque, NM, USA

Corresponding Author:
John J. Heifner, 8905 Southwest 87th Avenue, Miami, FL 33176, USA.
Email: johnjheifner@gmail.com

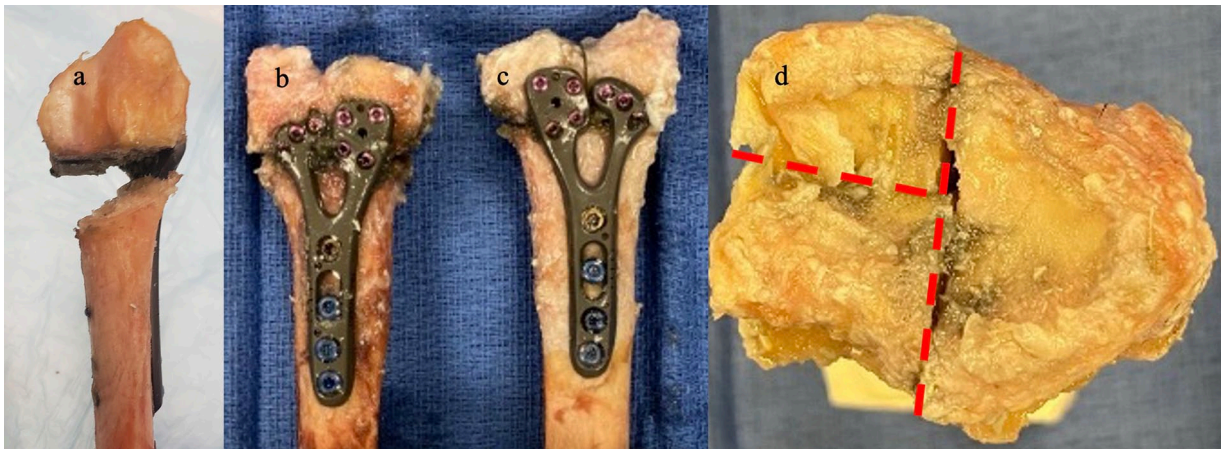

Figure 1. (a and b) Nonarticular and (c and d) articular fractures were created using a cutting jig for the dorsal wedge osteotomy that was made 1.5 cm proximal to the dorsal radial articular ridge.

The column concept of Rikli and Regazzoni provides a framework to understand distal radius fixation constructs.[15] The column concept states that after DRF, stability must always be restored to both the lateral and the intermediate columns. There is also consideration for stabilization of the third or medial column in the presence of an unstable distal radioulnar joint. The lateral and intermediate columns act as independent load-bearing structures.

The importance of postoperative rehabilitation following VLP fixation is well established.[16,17] Furthermore, recent evidence strengthens the value of mobilization that is initiated in the immediate postoperative period.[18-20] Satisfactory outcomes following these protocols are predicated on VLPs providing adequate stability to the fracture repair. Prior reports have biomechanically evaluated VLP stability in articular DRF patterns.[21-23] To our knowledge, the stability of a fossa-specific construct in articular DRF patterns has not been investigated. As VLP designs evolve, continued evidence is needed to evaluate the capabilities of these systems to accommodate immediate mobilization.[17]

Our objective was to compare fixation stability between articular and non-articular DRF patterns using a VLP which individually supports the lateral and intermediate radial columns. These fracture models were tested under loading parameters meant to simulate postoperative rehabilitation. We hypothesized that stability would be comparable between articular and non-articular fracture patterns.

Materials and Methods

Specimen Preparation

Using 6 matched pairs, a preliminary power analysis was done to determine appropriate sample size. This analysis indicated that 11 matched pairs were needed to demonstrate sufficient power. The power analysis was done using alpha = 0.05 and beta = 0.8. Across the 11 male matched pairs of fresh-frozen human cadaver forearms used in this study, the median age was 59 years (interquartile range = 11). Radiographs were obtained to ensure no prior trauma or arthritic changes. Specimens were thawed for 24 hours prior to initiating bony preparation. Each radius was removed from cadaveric forearms and osteotomized at the junction of the middle and distal third of the radial shaft. The hand was disarticulated at the radiocarpal joint. The radii were pinned and potted with urethane casting resin (Smooth-Cast 300, Smooth-On Inc, Macungie, Pennsylvania) for securing the radii to the test fixture.

A randomization procedure was used to identify one specimen from each pair to be included in the non-articular fracture pattern test group. The contra-lateral specimen was placed in the articular fracture pattern group. Care was taken to ensure a similar number of left and right radii in each group to avoid handedness bias. All fracture models were created by a fellowship trained hand surgeon. A 25 mm x 9.2 mm x 0.48 mm Casper oscillating saw blade (Stryker TPS, Kalamazoo, Michigan) and custom cutting jig were used to create the AO Type A2 nonarticular and the AO Type C3 multifragmentary articular fracture to ensure osteotomy consistency.[24] The non-articular model was created by first making a transverse cut 1.5 cm proximal to the distal articular surface. A second cut was made at 45 degrees in relation to the transverse cut, at 5 mm proximal to the distal articular surface, removing a 1 cm wedge of bone to simulate dorsal metaphyseal comminution. For the AO Type C3 multi-fragmentary articular fracture, an additional sagittal cut at the junction of the scaphoid and lunate facet, followed by a coronal cut in the center of the lunate fragment (Figure 1). In

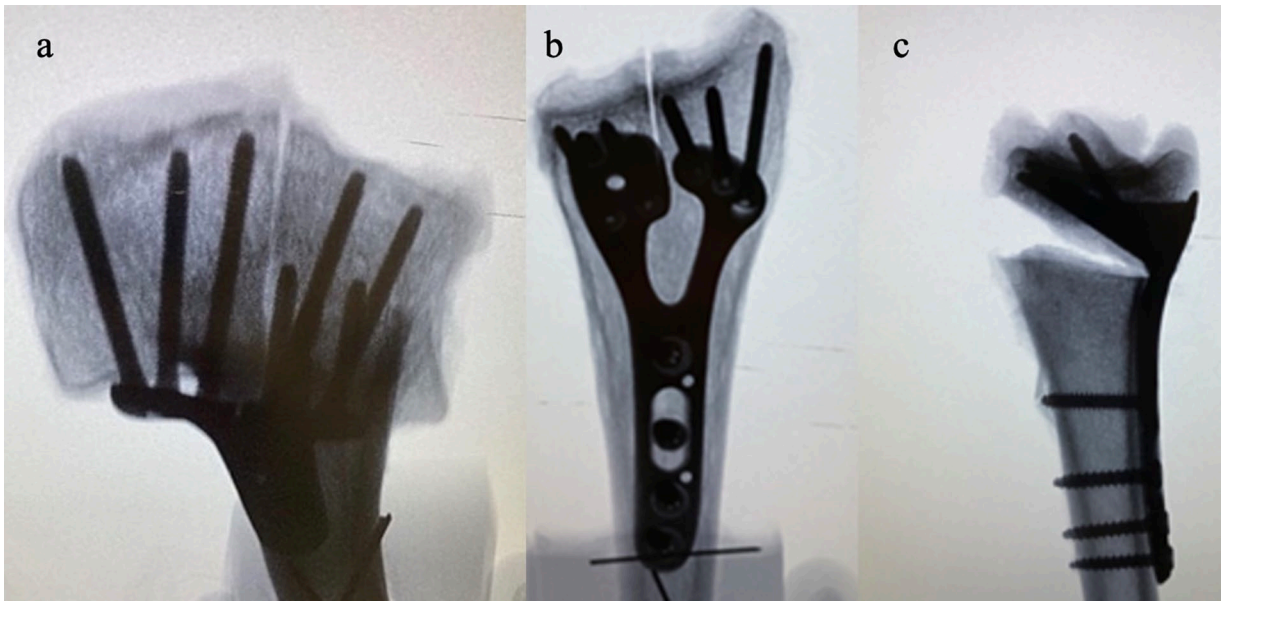

Figure 2. Extended (a) tangential, (b) anteroposterior, and (c) lateral view fluoroscopy with appropriate subchondral screw lengths in an articular fracture pattern.

both fracture models, we ensured the presence of a 2 mm gap with no contact of the volar cortical bone.

Implant Placement

The appropriately sized VLP was determined by maximizing the coronal plane coverage of the distal radius without plate overhang or screw cut-out. The VLP being tested was the Geminus (Skeletal Dynamics, Miami, Florida). This plate has a dual-column design which independently supports the lateral and intermediate columns of the distal radius with fixed-angle multi-planar points of fixation. In all fracture fixation, 2.3 mm threaded locking screws were used distally in the metaphysis and 3.5 mm fully threaded nonlocking cortical screws were used in the radius shaft. Technique for plate placement was consistent for the articular and nonarticular groups. The distal edge of each plate was placed approximately 2 mm proximal to the watershed line, an anatomical landmark which is defined by the volar rim of the lunate fossa. The proximal end of the plate was positioned colinear with the radial shaft. A non-locking screw was first placed in the shaft gliding hole. Kirchner wires (K-wires) were placed in the most proximal ulnar 2.3 mm screw hole and the radial styloid 2.3 mm screw hole using a K-wire guide. This stabilized the distal fracture fragments. Anteroposterior, 30 degrees lateral and extended tangential fluoroscopic views were used to confirm appropriate plate width and k wire position. The K wires, shaft screw and plate were then removed. The osteotomy was created as described above, and the plate was replaced by first placing the K-wires in the distal fragment followed by securing the plate to the shaft. The remaining shaft screw holes were filled by first predrilling, then measuring, then placing the correct size screw. Fixation of the distal fragment(s) consisted of bicortical drilling then placing screws which measured 2 mm shorter than measured length to ensure no dorsal cortical breech. Anteroposterior, 30 degrees lateral and extended tangential fluoroscopic views were used to confirm correct screw length and plate position. The distal screws did not project past the dorsal cortex (Figure 2).

Experimental Testing

Matched articular and nonarticular DRF fixation constructs were tested under cyclic loading. A Mini Bionix servohydraulic load frame was used for testing (MTS Systems, Eden Prairie, Minnesota). The proximal potted block was fixed to the actuator in line with the radial shaft. An angled vise and custom fixture allowed a 60/40 load distribution to be applied to the scaphoid and lunate facets respectively (Figure 3).[25] The loading parameters were previously described to simulate postoperative rehabilitation loads following DRF fixation.[26] Specimens were preloaded to 50 N for 30 seconds then were sinusoidally compressed from 50 to 250 N at 1 Hz for 5000 cycles to simulate light active weight bearing during the immediate postoperative period.[26]

Figure 3. Application of axial load with 60/40 distribution (lunate/scaphoid facets respectively) via an angled vise.

Outcome Measure and Statistical Analysis

The outcome measure was the stiffness of bone/implant constructs (slope of the most linear region of the force/displacement curve) during cyclic loading.

Data columns were tested for normality with Shapiro Wilk tests. Data analyses were completed using R® software. A 1-tailed, matched paired Student *t*-test was used to determine statistical significance at an alpha level of 0.05 between the articular and non-articular fracture pattern groups.

Results

Mean stiffness for non-articular specimens was 370.0 N (+/-93.5), and mean stiffness for articular specimens was 360.4 N (+/-60.0). Differences were not statistically significant when comparing the articular and non-articular models ($P = .35$) (Table 1). Individual specimen results for both articular and non-articular fracture models are shown in Table 2.

Discussion

There is increasing evidence for accelerated recovery when rehabilitation is performed immediately following DRF fixation.[18-20,27] The momentum for immediate postoperative rehabilitation highlights the importance of the stability provided by VLP constructs.[17] Under cyclic loading meant to simulate postoperative rehabilitation demands, results showed no significant difference in construct stiffness between the articular and non-articular fracture patterns. The current findings demonstrate that a VLP with individual support for the distal radius columns can provide appropriate levels of stability in articular fracture patterns. Importantly, the levels of stability were recorded under loading parameters that simulate postoperative rehabilitation.

Recent biomechanical studies on VLP fixation have utilized loading parameters meant to simulate postoperative function. Marshall et al[28] compared VLP composition in a C3 DRF model using cyclic loading from 20 N to 230 N for 6000 cycles. Salas et al[26] compared VLP designs in an A3 DRF model using cyclic loading from 50 N to 250 N for 5000 cycles. When comparing 1 row to 2 rows of distal screws in a VLP, Tsutsui et al[29] used a C2 DRF model under cyclic loading from 0 to 250 N for 3000 cycles. Our protocol of cyclic loading from 50 N to 250 N for 5000 cycles is similar in load and cycles to the recent literature.

The column concept of loading onto the distal radius is corroborated by observations of bony and fracture anatomy. The scaphoid fossa or lateral column is supported by 2 cancellous bone units that transmit load to the dorsal and palmar radial cortexes. The scaphoid fossa remains a single fragment in many articular injuries. The lunate fossa is supported by a single palmar cancellous bone unit which primarily transmits loads to the palmar cortex. The lunate fossa is commonly divided into 2 fragments by a coronal fracture line. The column concept can be applied to VLPs as these devices can fulfill the fixation requirements of both lateral and intermediate columns. This capability is predicated on the locking screws being properly positioned to create the rafting construct that is required by the unique anatomy of each column or fossae. The intermediate column requires subchondral support to the dorsal and palmar aspects due to several factors. Common articular fracture patterns have a coronal fracture plane that divides the lunate fossa into a palmar and a dorsal fragment.[12] The lunate fossa has a more palmarly located centroid of force application when the wrist is neutral[25,30,31] and the fossa is offset palmarly from the radial shaft.[32] Additionally, the concave surface of the distal radius accounts for the planar variation between the dorsal and volar articular surfaces of the lunate fossa. Thus, subchondral rafting support of these fragments requires 2 or more elements that cross in the coronal plane and are tangential to the dorsal and volar articular surface. This construct is intended to reproduce the concave geometry of the distal radius articular surface. The scaphoid fossa, because of its greater volar tilt[33] and its centrally located centroid of force application,[30] can be effectively supported by a single plane of subchondral support elements. The concept of independent column

Table 1. Stiffness Comparison Between Articular and Non-Articular Distal Radius Fracture Patterns.

N = 11	Articular fracture patterns	Non-articular fracture patterns	Statistical significance
Stiffness			
Mean	360.4 N/mm	370.0 N/mm	$P = .35$
SD	60.0	99.5	

Table 2. Stiffness Values for Individual Specimens in Articular and Non-Articular Distal Radius Fracture Patterns.

	Stiffness		
Specimen	Articular fracture patterns (N/mm)	Non-articular fracture patterns (N/mm)	Difference
1	425.2	391.3	33.9
2	339.7	467.6	(127.9)
3	316.2	217.9	98.3
4	323.6	351.0	(27.4)
5	300.2	296.1	4.1
6	301.8	401.1	(99.3)
7	465.7	517.4	(51.7)
8	350.4	317.6	32.8
9	450.0	453.2	(3.2)
10	372.1	248.8	123.3
11	319.3	407.0	(87.7)

buttressing was developed due to an understanding of the loading mechanics on the distal radius.[15,34] This biomechanical principle has been applied to fragment-specific fixation and to VLP design.

Stiffness of the fixation construct is an integral component for bone healing. Articular fragmentation and displacement may preclude some fixation methods and constructs from maintaining reduction or facilitating bone healing.[35,36] Fracture healing is dependent upon mechanical stability and vascularization. Mechanical stability refers to the likelihood of fracture fragments to remain in the reduced position. Stiffness is an aspect of stability that refers to the force needed to displace the fragments a unit of length. Higher stiffness reduces the potential for interfragmentary motion and displacement. In the case of articular fragment vascular disruption which can occur with a volar marginal fragment, greater stiffness may be needed for healing to occur.[10,37-39]

Limitations of the current work include those that are inherent to biomechanical testing. Cadavers have variable bone density, and the biological tissue is not consistent across specimens. Matched pairs were used to minimize this error. We did not have data for specimen handedness. Though given the current sample size and the population distribution of hand dominance, it is unlikely that these data would have influenced the results. The conclusions were derived from comparison of 2 specific fracture patterns, therefore may not be generalizable to other fracture patterns. Additionally, the use of a single VLP reduces the applicability of the conclusions to constructs featuring other locking plate designs. The conclusion demonstrates the biomechanical capability of a fossa specific VLP to accommodate postoperative loading following a comminuted articular DRF. Future study is needed to determine if these findings are clinically supported. Strengths of the work include a single implant design and previously validated loading parameters meant to simulate postoperative loading.

Our findings demonstrate that a VLP which individually supports the scaphoid and lunate fossa with fixed angle subchondral support may provide comparable fixation stability with resistance to displacement between non-articular and articular fracture patterns under loading parameters meant to simulate post-operative rehabilitation.

Ethical Approval

This study was approved by our institutional review board.

Statement of Human and Animal Rights

This article does not contain any studies on human or animal subjects.

Statement of Informed Consent

This article does not contain any studies on human or animal subjects.

Declaration of Conflicting Interests

The author(s) declared the following potential conflicts of interest with respect to the research, authorship, and/or publication of this article: D.M. declares speakers bureau relationship with Skeletal Dynamics and Axogen. J.H., N.M., and C.S. have nothing to declare.

Funding

The author(s) disclosed receipt of the following financial support for the research, authorship, and/or publication of this article: The devices used for this work were provided through a material transfer agreement with Skeletal Dynamics, LLC. The author(s) received no financial support for the research, authorship and/or publication of this article.

ORCID iD

John J. Heifner https://orcid.org/0000-0001-6034-6677

References

1. Department of Economic and Social Affairs, United Nations. World population ageing 2019: highlights (ST/ESA/SER.A/430). https://www.un.org/en/development/desa/population/publications/pdf/ageing/WorldPopulationAgeing2019-Highlights.pdf. Published 2019. Accessed August 26, 2022.
2. Corsino CB, Reeves RA, Sieg RN. Distal radius fractures. In: *StatPearls*. Treasure Island, FL: StatPearls Publishing; 2022.
3. American Academy of Orthopaedic Surgeons. Management of distal radius fractures evidence-based clinical practice guideline. Date unknown. http://www.aaos.org/drfcpg. Accessed August 26, 2022.
4. Rundgren J, Bojan A, Mellstrand Navarro C, et al. Epidemiology, classification, treatment and mortality of distal radius fractures in adults: an observational study of 23,394 fractures from the national Swedish fracture register. *BMC Musculoskelet Disord*. 2020;21(1):88.
5. Sander AL, Leiblein M, Sommer K, et al. Epidemiology and treatment of distal radius fractures: current concept based on fracture severity and not on age. *Eur J Trauma Emerg Surg*. 2020;46(3):585-590.
6. Stephens AR, Presson AP, McFarland MM, et al. Volar locked plating versus closed reduction and casting for acute, displaced distal radial fractures in the elderly: a systematic review and meta-analysis of randomized controlled trials. *J Bone Joint Surg Am*. 2020;102(14):1280-1288.
7. Woolnough T, Axelrod D, Bozzo A, et al. What is the relative effectiveness of the various surgical treatment options for distal radius fractures? A systematic review and network meta-analysis of randomized controlled trials. *Clin Orthop Relat Res*. 2021;479(2):348-362.
8. Gou Q, Xiong X, Cao D, et al. Volar locking plate versus external fixation for unstable distal radius fractures: a systematic review and meta-analysis based on randomized controlled trials. *BMC Musculoskelet Disord*. 2021;22(1):433.
9. Saving J, Severin Wahlgren S, Olsson K, et al. Nonoperative treatment compared with volar locking plate fixation for dorsally displaced distal radial fractures in the elderly: a randomized controlled trial. *J Bone Joint Surg Am*. 2019;101(11):961-969.
10. Heifner JJ, Orbay JL. Assessment and management of acute volar rim fractures. *J Wrist Surg*. 2022;11:214-218.
11. Souer JS, Ring D, Jupiter J, et al. Comparison of intra-articular simple compression and extra-articular distal radial fractures. *J Bone Joint Surg Am*. 2011;93(22):2093-2099.
12. Zhou J, Tang W, Li D, et al. Morphological characteristics of different types of distal radius die-punch fractures based on three-column theory. *J Orthop Surg Res*. 2019;14(1):390.
13. Melone CP Jr. Distal radius fractures: patterns of articular fragmentation. *Orthop Clin North Am*. 1993;24(2):239-253.
14. Teunis T, Bosma NH, Lubberts B, et al. Melone's concept revisited: 3D quantification of fragment displacement. *J Hand Microsurg*. 2016;8(1):27-33.
15. Rikli DA, Regazzoni P. Fractures of the distal end of the radius treated by internal fixation and early function. *J Bone Joint Surg Br*. 1996;78(4):588-592.
16. Gamo K, Baba N, Kakimoto T, et al. Efficacy of hand therapy after volar locking plate fixation of distal radius fracture in middle-aged to elderly women: a randomized controlled trial. *J Hand Surg Am*. 2022;47(1):62.e1-e67.
17. Quadlbauer S, Pezzei C, Jurkowitsch J, et al. Rehabilitation after distal radius fractures: is there a need for immobilization and physiotherapy. *Arch Orthop Trauma Surg*. 2020;140(5):651-663.
18. Quadlbauer S, Pezzei C, Jurkowitsch J, et al. Immediate mobilization of distal radius fractures stabilized by volar locking plate results in a better short-term outcome than a five week immobilization: a prospective randomized trial. *Clin Rehabil*. 2022;36(1):69-86.
19. Lee JK, Yoon BH, Kim B, et al. Is early mobilization after volar locking plate fixation in distal radius fractures really beneficial? a meta-analysis of prospective randomized studies [published online ahead of print December 2021]. *J Hand Ther*. doi:10.1016/j.jht.2021.10.003.
20. Gutierrez-Espinoza H, Araya-Quintanilla F, Olguin-Huerta C, et al. Effectiveness of early versus delayed motion in patients with distal radius fracture treated with volar locking plate: a systematic review and meta-analysis. *Hand Surg Rehabil*. 2021;40(1):6-16.
21. Rausch S, Klos K, Stephan H, et al. Evaluation of a polyaxial angle-stable volar plate in a distal radius C-fracture model–a biomechanical study. *Injury*. 2011;42(11):1248-1252.
22. Stanbury SJ, Salo A, Elfar JC. Biomechanical analysis of a volar variable-angle locking plate: the effect of capturing a distal radial styloid fragment. *J Hand Surg Am*. 2012;37(12):2488-2494.
23. Kamei S, Osada D, Tamai K, et al. Stability of volar locking plate systems for AO type C3 fractures of the distal radius: biomechanical study in a cadaveric model. *J Orthop Sci*. 2012;15(3):357-364.
24. Dahl WJ, Nassab PF, Burgess KM, et al. Biomechanical properties of fixed-angle volar distal radius plates under dynamic loading. *J Hand Surg Am*. 2012;37(7):1381-1387.
25. Majima M, Horii E, Matsuki H, et al. Load transmission through the wrist in the extended position. *J Hand Surg Am*. 2008;33(2):182-188.

26. Salas C, Brantley JA, Clark J, et al. Damage in a distal radius fracture model treated with locked volar plating after simulated postoperative loading. *J Hand Surg Am*. 2018;43(7):679.e1-e676.
27. Brehmer JL, Husband JB. Accelerated rehabilitation compared with a standard protocol after distal radial fractures treated with volar open reduction and internal fixation: a prospective, randomized, controlled study. *J Bone Joint Surg Am*. 2014;96(19):1621-1630.
28. Marshall T, Momaya A, Eberhardt A, et al. Biomechanical comparison of volar fixed-angle locking plates for AO C3 distal radius fractures: titanium versus stainless steel with compression. *J Hand Surg Am*. 2015;40(10):2032-2038.
29. Tsutsui S, Kawasaki K, Yamakoshi K, et al. Impact of double-tiered subchondral support procedure with a polyaxial locking plate on the stability of distal radius fractures using fresh cadaveric forearms: biomechanical and radiographic analyses. *J Orthop Sci*. 2016;21:603-608.
30. Viegas SF, Tencer AF, Cantrell J, et al. Load transfer characteristics of the wrist. Part I. The normal joint. *J Hand Surg Am*. 1987;12(6):971-978.
31. Tang P, Gauvin J, Muriuki M, et al. Comparison of the "contact biomechanics" of the intact and proximal row carpectomy wrist. *J Hand Surg Am*. 2009;34(4):660-670.
32. Andermahr J, Lozano-Calderon S, Trafton T, et al. The volar extension of the lunate facet of the distal radius: a quantitative anatomic study. *J Hand Surg Am*. 2006;31(6):892-895.
33. Gasse N, Lepage D, Pem R, et al. Anatomical and radiological study applied to distal radius surgery. *Surg Radiol Anat*. 2011;33(6):485-490.
34. Jupiter JB, Lipton H. The operative treatment of intraarticular fractures of the distal radius. *Clin Orthop Relat Res*. 1993;292:48-61.
35. Perren SM. Physical and biological aspects of fracture healing with special reference to internal fixation. *Clin Orthop Relat Res*. 1979;138:175-196.
36. Perren SM, Cordey J. The concept of interfragmentary strain. In: Uhthoff HK, Stahl E, eds. *Current Concepts of Internal Fixation of Fractures*. New York, NY: Springer; 1980:63-77.
37. Ruedi TP, Murphy WM. *AO Principles of Fracture Management*. Stuttgart, Germany: Thieme; 2000.
38. Lienau J, Schell H, Duda GN, et al. Initial vascularization and tissue differentiation are influenced by fixation stability. *J Orthop Res*. 2005;23(3):639-645.
39. Harness NG, Jupiter JB, Orbay JL, et al. Loss of fixation of the volar lunate facet fragment in fractures of the distal part of the radius. *J Bone Joint Surg Am*. 2004;86(9):1900-1908.